Power System Transient Stability Analysis with Integration of DFIGs Based on Center of Inertia

Siwei Liu, Gengyin Li, *Member, IEEE*, and Ming Zhou, *Member, IEEE*

***Abstract*—As power systems experience increased wind penetration, an effective analysis and assessment of the influence of wind energy on power system transient stability is required. This paper presents a novel center of inertia (COI) approach to understand how integrated doubly fed induction generators (DFIGs) affect the transient dynamics of a power system. Under the COI coordinate, the influence of integrated DFIGs is separated into the COI related and individual synchronous generator related parts. Key factors that affect the COI's dynamic motion as well as the rotor dynamics of each individual synchronous generator with respect to the DFIG integration are investigated. To further validate the analysis, comparative simulations of three different scenarios with varying DFIG capacities, access locations, and the replacement of synchronous generators are conducted. The results show that the dynamics of the COI and the individual generators are affected by the integrated DFIGs via different mechanisms, and are sensitive to different variables in the DFIG's integration condition.**

***Index Terms*—Center of inertia (COI), doubly fed induction generator (DFIG), influence mechanism, motion equation, power system transient stability, rotor dynamics.**

I. Introduction

POWER generation from renewable energies, such as wind, has become recognized worldwide as an effective method to achieve sustainable development in economic and environmental terms. In 2014, the cumulative installed capacity of wind power in China reached 114.609 GW. Among different wind power generators, the doubly fed induction generator (DFIG) has become a mainstream technology with mature development and full utilization mainly due to its high energy efficiency, reduced mechanical stress on wind turbines, and the relatively low power rating of its electronics converters [1]–[3].

However, with the converters used in the DFIG's excitation system, the dynamic response of the DFIG is mainly dependent on the coordinated control strategies of the converters, which are essentially different from traditional synchronous generators [4], [5]. With increasing DFIG-based wind power penetration, the systematic and effective evaluation of the influence of integrated DFIGs on power system transient stability has become a prominent issue and needs to be clearly explored.

Considerable literature is available on the influence of DFIG integration on power system transient stability [6]–[18]. In early works, the studies mostly focused on the use of simulation methods [9]–[13]. The study in [9] observed the influence of integrated DFIGs on the rotor dynamics of synchronous generators based on a two-generator to infinite system. The work in [10] considered the variables of different DFIG penetrations, network structures, and points of common coupling (PCC) for assessing the influence of integrated DFIGs on the system's transient dynamics. In [11] utilization of synchrophasor measurements was explored to estimate the equivalent inertia of a power source such as synchronous generators or wind turbine generators for detecting the angle instability of a system with wind power penetration.

As a complement for simulation analysis, different transient stability indices have been proposed and utilized [10]–[18], with the fault critical clearing time (CCT) being the most widely adopted index [10]–[12], [14]. In [14], the CCT of a CIGRE 39 bus system that integrated both DFIGs and synchronous generators was simulated. The results showed that DFIGs improved the robustness of the system. In other studies, different transient stability indices have also been proposed and investigated [15]–[18]. In [15], a transient stability index (TSI), calculated by the maximum angle deviation of any two synchronous generators in the system, was introduced. By considering different DFIG integration conditions, it was pointed out that the influence of DFIGs on the transient stability of the system could be both positive and negative. In [16], a modified transient energy function (TEF) was proposed to evaluate the influence of integrated wind turbine generators on the whole system's transient stability margin. The results showed that the synchronous generators possess a higher transient stability value, implying more favorable transient behavior than that of wind turbine generators.

As mentioned above, a number of achievements have analyzed the influence of integrated DFIGs on the transient stability of either the overall system or individual synchronous generators. Different DFIG integration conditions have also been widely considered with different system models. However, there has been no agreement in the research community on whether the influence of integrated DFIGs on the system's transient stability is detrimental or beneficial, partly because

Manuscript received December 15, 2015; revised February 20, 2016; accepted April 5, 2016. Date of publication June 30, 2016; date of current version May 3, 2016. This work was supported in part by the Major Program of the National Natural Science Foundation of China under Grant 51190103, and the National High Technology Research and Development Program of China under Grant 2012AA050208.

S. W. Liu (corresponding author, e-mail: liusw@ncepu.edu.cn), G. Y. Li, and M. Zhou are with State Key Laboratory of Alternate Electrical Power System with Renewable Energy Sources, North China Electric Power University, Beijing 102206, China.

DOI: 10.17775/CSEEJPES.2016.00018

the mechanisms causing the simulated results have not yet been comprehensively investigated. Therefore, there is a need for a deeper mechanistic analysis, which reflects the general rules of the influence of integrated DFIGs on transient stability.

In the transient stability analysis of multi-machine systems, the system center of inertia (COI), which is described as an assumed dynamic position measured by the weighted average of the instantaneous rotor angle of all the synchronous generators in the system, has been widely used for various specific objectives and approaches [19]–[22]. COI, first introduced in [23] by Stewart, can well represent the dynamic behaviors of an overall system and its coherent generator clusters [24]. The COI-based coordinate is also an effective index for monitoring the dynamics of individual synchronous generator with respect to the general trend of the global system [25].

In this paper, instead of trying to make a definitive judgment on whether the influence of the integrated DFIGs on system transient stability is positive or negative, we aim to provide a better understanding of its influence mechanism. The contributions are summarized as follows.

1) The characteristic of the DFIG's transient behavior is analyzed, which is the basis for re-formulating the system models by taking into consideration the influence of integrated DFIGs under the COI coordinate.
2) Based on the developed formulations, the impact of DFIG integration on the COI's dynamic motion and each individual synchronous generator's rotor dynamics with respect to the COI are investigated. The possible variations in the key factors that affect the dynamics of the COI and individual generators are also taken into account in the analysis.
3) The time-domain simulation studies provide a validation for the previous analysis and present concrete insights into how the different DFIG integration conditions influence the system's transient behaviors.

The remainder of this paper is organized as follows: Section II describes the DFIG models and discusses the transient response characteristics of DFIGs. Section III establishes the basic COI models. Section IV re-formulates the system model based on COI factoring in the integrated DFIG's impact, and then examines its effect on the COI related part and individual synchronous generator related parts. Section V describes simulations that compare three different scenarios in varying DFIG capacities, access locations, and synchronous generator replacements. Section VI summarizes the study.

II. Transient Behavior Analysis of DFIG

It is important to understand the difference in transient behavior characteristics of integrated DFIGs when compared to conventional synchronous generators, particularly when investigating the influence mechanism of integrated DFIGs on power system transient stability.

During a system disturbance, traditional synchronous generators accelerate or decelerate due to a mismatch in input mechanical power and output electrical power. As a result of the difference between the generator rotor speed and grid frequency, the change in rotor angle leads to variations in the electrical power output based on the power angle characteristic in return. The synchronous generator's inertia plays a role in suppressing the rapid changes in rotor speed and electrical power output; it is also responsible for damping the oscillation of grid frequency. Hence, the power generation of synchronous generators has a tight relationship with the rotor speed and system frequency.

In the case of DFIGs, however, the back-to-back converters provide a fast and accurate variable-frequency excitation in a DFIG's rotor windings such that the electrical variables in stator windings are always able to keep within the same angular speed of the grid regardless of how the rotor speed changes. Owing to this fact, the electrical power outputs of integrated DFIGs are electro-mechanically decoupled from the rotor dynamics and thus can be modulated quickly and flexibly during system disturbance. Hence, the integrated DFIGs are mostly regarded as providing no contribution to the power system inertia [26]. Also, the concepts of "relative swing" and "rotor angle deviation" are not suitable for describing the relationship between the integrated DFIGs and synchronous generators since the power angle characteristic does not exist in the DFIG's excitation.

It is suggested, therefore, that during power system transients, integrated DFIG-based wind turbine generators operate independently without direct interactions with other generators in the system. They only suffer from low voltage ride through (LVRT), which in turn depends on terminal voltage dynamics and the operating conditions of the converters.

It is also important to note that since integrated DFIGs are normally required to operate at maximum power tracking (MPT) mode to generate more active power, the reactive power output is deemed rather small [5]. Even if the DFIG is controlled to send reactive power to the grid during grid fault, its grid voltage will still be much smaller when compared to the conventional synchronous generator [27].

III. Mathematical Models of COI

Described as the center of rotor angles and rotor speeds of the synchronous generators in the system, the COI is defined as

$$\delta_{\mathrm{COI}} = \frac{1}{T_{\mathrm{J,COI}}}\left(\sum_{i=1}^{n} T_{\mathrm{J},i}\delta_i\right) \tag{1}$$

$$\omega_{\mathrm{COI}} = \frac{1}{T_{\mathrm{J,COI}}}\left(\sum_{i=1}^{n} T_{\mathrm{J},i}\omega_i\right) \tag{2}$$

where

$$T_{\mathrm{J,COI}} = \sum_{i=1}^{n} T_{\mathrm{J},i} \tag{3}$$

where δ and ω are the rotor angle and rotor speed, and T_{J} is the inertia constant. The subscript COI stands for the variable of the COI and subscript i denotes the variables of the i^{th} generator.

The motion equation of the COI is given by

$$p(\omega_{\mathrm{COI}}) = \frac{1}{T_{\mathrm{J,COI}}} P_{\mathrm{COI}} \tag{4}$$

where p is the differential algorithm; P_{COI} is defined as

$$P_{\mathrm{COI}} = P_{\mathrm{m,COI}} - P_{\mathrm{e,COI}} = (\sum_{i=1}^{n} P_{\mathrm{m},i}) - (\sum_{i=1}^{n} P_{\mathrm{e},i}) \quad (5)$$

where P_{m} is the mechanical power and P_{e} is the electrical power.

Based on (1) and (2), the dynamics of the i^{th} generator in the COI-based reference are expressed by

$$\delta_i^{\mathrm{COI}} = \delta_i - \delta_{\mathrm{COI}} \quad (6)$$

$$\omega_i^{\mathrm{COI}} = \omega_i - \omega_{\mathrm{COI}} \quad (7)$$

where the superscript COI represents the variables in the COI-based reference.

Based on (7)–(10), the dynamic motion equation of each synchronous generator in the COI-based reference is

$$\begin{aligned} p(\omega_i^{\mathrm{COI}}) &= p(\omega_i) - p(\omega_{\mathrm{COI}}) \\ &= \frac{1}{T_{\mathrm{J},i}}(P_{\mathrm{m},i} - P_{\mathrm{e},i}) - \frac{1}{T_{\mathrm{J,COI}}} P_{\mathrm{COI}}. \end{aligned} \quad (8)$$

IV. Transient Stability Analysis with DFIG Integration

From (1)–(8), it can be seen that the concept of COI is based on the synchronous generators' power angle characteristics and the mutual synchronization mechanism among synchronous generators. However, according to the transient behavior analysis of integrated DFIG carried out in Section II, it can be inferred that integrated DFIGs do not directly participate in the composition of COI, but may change the key factors that determine the transient behaviors of the COI and each synchronous generator with respect to the COI. Based on this, the influence of the integrated DFIGs on the dynamics of the COI and the individual synchronous generator with respect to the COI are both considered and analyzed under the COI coordinate in this work.

A. Influence of Integrated DFIGs on COI's Transient Dynamics

With DFIGs integrated, the dynamic motion equation of COI is given by

$$p(\omega'_{\mathrm{COI}}) = \frac{1}{T'_{\mathrm{J,COI}}}(P'_{\mathrm{m,COI}} - P'_{\mathrm{e,COI}}) \quad (9)$$

where superscript $'$ denotes the variables with DFIGs integrated.

As expressed in (9), with DFIGs integrated, the changes in the COI's inertia constant $T_{\mathrm{J,COI}}$, mechanical power $P_{\mathrm{m,COI}}$, and electrical power $P_{\mathrm{e,COI}}$ collectively determine the influence on the motions of system COI. To investigate how the integrated DFIGs affect the COI's dynamics, the impacts of integrated DFIGs on these three factors need to be first investigated.

1) Impacts on $T_{\mathrm{J,COI}}$

Considering that the integrated DFIGs are regarded as non-inertia to the grid, $T_{\mathrm{J,COI}}$ would not be changed if DFIGs are integrated without replacing any synchronous generators, where $T'_{\mathrm{J,COI}} = T_{\mathrm{J,COI}}$. However, when DFIGs are integrated by replacing some synchronous generators, the $T_{\mathrm{J,COI}}$ then should be described by

$$T'_{\mathrm{J,COI}} = T_{\mathrm{J,COI}} - T_{\mathrm{J,rep}} \quad (10)$$

where $T_{\mathrm{J,rep}}$ is the inertia constant of the replaced synchronous generators.

2) Impacts on $P_{\mathrm{m,COI}}$

For both the synchronous generators and DFIGs, the governors are unable to regulate the mechanical power rapidly during a system transient. Therefore, P_{m} is usually regarded as a constant value in theoretical transient analysis for simplification. Hence, the mechanical power of the synchronous generators, the DFIGs and the COI in this work are also considered unchanged during system transients as well. And the COI mechanical power can be described by

$$\begin{cases} P_{\mathrm{m,COI}} = P_{\mathrm{e,COI},|0|} = P_{\Sigma,|0|} \\ P'_{\mathrm{m,COI}} = P'_{\Sigma,|0|} - P_{\mathrm{m,DFIG}} \end{cases} \quad (11)$$

with

$$P_{\Sigma} = P_{\mathrm{load},\Sigma} + P_{\mathrm{loss},\Sigma} \quad (12)$$

where $P_{\mathrm{load},\sum}$, $P_{\mathrm{loss},\sum}$ and $P_{\sum}$ are the total loads, total loss and total power demand of the system, respectively. The subscript $|0|$ denotes the variables at the pre-fault state.

3) Impacts on $P_{\mathrm{e,COI}}$

The output electrical power of an individual generator is time-variant depending on its operation state, however, the total amount of all the generators' output electrical power in a system always equals to the total dynamic power demand in the system. Thus, the COI electrical power $P_{\mathrm{e,COI}}$ and $P'_{\mathrm{e,COI}}$ can be described as

$$\begin{cases} P_{\mathrm{e,COI}} = P_{\Sigma} \\ P'_{\mathrm{e,COI}} = P'_{\Sigma} - P_{\mathrm{e,DFIG}}. \end{cases} \quad (13)$$

The dynamic response of system total power demand which consists of $P_{\mathrm{load},\sum}$ and $P_{\mathrm{loss},\sum}$, is largely determined by the system voltage stability. Thus, if in the situation where the transient voltage dynamic of the system is not significantly affected by integrated DFIGs, the dynamics of $P'_{\sum}$ can be regarded being the same as that of $P_{\sum}$ under the same system disturbance, expressed as

$$P'_{\Sigma} \approx P_{\Sigma}. \quad (14)$$

However, if the network structures or the reactive power distribution is obviously influenced by DFIG integration and the changes in system transient voltage stability need to be considered, the dynamic response of $P'_{\sum}$ would not equal to that of $P_{\sum}$.

The dynamic response of the integrated DFIGs' electrical power output, $P_{\mathrm{e,DFIG}}$ is another key factor affecting the dynamics of $P'_{\mathrm{e,COI}}$, according to (13). As analyzed previously, the dynamic response of $P_{\mathrm{e,DFIG}}$ is significantly different from that of synchronous generators due to the different excitation mechanisms. Thus, if the dynamic response of system total demand $P'_{\sum}$isn't much influenced by DFIG integration, the

difference between $P'_{\mathrm{e,COI}}$ and $P_{\mathrm{e,COI}}$ would be totally determined by the dynamic response of the integrated DFIGs' electrical power output.

The COI inertia constant is the intrinsic character of the power system, which does not change during dynamic operations. The COI mechanical power also remains unchanged during the transient process, as well. Only the COI electrical power is time-variant during the transient process. However, how would these three key factors exactly change with DFIG integration, and how the variations of these factors affect the COI's dynamics, all depend on the specific integration conditions of the DFIGs.

B. Influence of Integrated DFIGs on Individual Synchronous Generator's COI-referred Transient Dynamics

The influence of the integrated DFIGs on the transient trajectories of each individual synchronous generator is not only embodied in the rotor motion dynamics, but also in the rotor angle states. The COI-referred dynamic motion reflects the rotor kinetic energy with respect to the overall system's variation trend, and the COI-referred rotor angles of each synchronous generator is an indicator of the changes in the rotor potential energy with respect to the dynamic center of the system.

The dynamic motion of the i^{th} synchronous generator with respect to COI with DFIGs integrated is described as

$$p(\omega_i^{\mathrm{COI}'}) = \frac{1}{T_{\mathrm{J},i}}(P'_{\mathrm{m},i} - P'_{\mathrm{e},i}) - p(\omega'_{\mathrm{COI}}). \tag{15}$$

Based on (7) and (15), the change in the i^{th} synchronous generator's dynamic motion can be described as

$$p(\omega_i^{\mathrm{COI}\prime}) - p(\omega_i^{\mathrm{COI}}) = \frac{1}{T_{\mathrm{J},i}}\left[(P_{\mathrm{m},i} - P_{\mathrm{e},i}) - (P'_{\mathrm{m},i} - P'_{\mathrm{e},i})\right] + \left[p(\omega_{\mathrm{COI}}) - p(\omega'_{\mathrm{COI}})\right]. \tag{16}$$

According to (16), the influence of integrated DFIGs on the dynamic motion of each individual synchronous generator with respect to the COI is determined by the changes in both the transient dynamics of the synchronous generator itself and the COI's motion. The changes in the COI's dynamic motion with DFIG integration have been analyzed previously. The dynamic motion of the synchronous generator is affected by the changes in $P_{\mathrm{m},i}$ and $P_{\mathrm{e},i}$. Before fault, $P'_{\mathrm{m},i}$ and $P'_{\mathrm{e},i|0|}$ of the synchronous generators are already different from $P_{\mathrm{m},i}$ and $P_{\mathrm{e},i|0|}$, since the system power flow has been inevitably changed with DFIG integration. $P'_{\mathrm{m,i}}$ and $P'_{\mathrm{e},i|0|}$ of each individual synchronous generator has reached new operating states to meet new power balance. When faults occur, considering that the dynamic response of $P_{\mathrm{e,DFIG}}$ is different from that of the synchronous generators in the system, the electrical power output $P'_{\mathrm{e},i}$ of each individual synchronous generator would have a more different dynamic response.

The rotor angle of each synchronous generator with respect to the COI with DFIG integration is written as

$$\delta_i^{\mathrm{COI}'} = \delta'_i - \delta'_{\mathrm{COI}}. \tag{17}$$

The variation in the rotor angle states of each synchronous generator directly indicates the operation states of the generator. Typically, if a synchronous generator's electrical power output is shared by the integrated DFIGs, it will have a lower value of $\delta'_{i,|0|}$ at pre-fault state. When faults occur, the dynamic response of δ'_i varies depending on the power-angle characteristics, the generator inertia constant $T_{\mathrm{J},i}$, and the dynamic response of $P'_{\mathrm{e},i}$. To some extent, the dynamic response of the rotor angle reflects the variations in the dynamics of the rotor speed.

This suggests that for each individual synchronous generator, the variation in its accelerating power, $(P'_{\mathrm{e},i} - P_{\mathrm{m},i})$, plays a very important role in affecting the dynamic response of both the rotor speed and rotor angle with DFIG integration. However, considering that the changes in COI's dynamic motions also need to be accounted for, it is clear that the influence of integrated DFIGs on the transient dynamic of each individual synchronous generator with respect to the COI is still complex, requiring further simulation analysis.

V. Simulations and Results Analysis

A modified IEEE 3 Gen-9 bus power system is adopted for the following simulation studies, as shown in Fig. 1. Synchronous generators with governor and excitation controls are used to initially model the three generators. The power loads are represented by constant impedance models to minimize the effect of the load's dynamic characteristics. An aggregated DFIG model whose parameters are calculated by the weighted equivalent method represents the integrated DFIG-based wind farm (DFIG-WF) [28]. Considering the purpose of this investigation, the integrated DFIG-WF is assumed to operate at the MPT mode that delivers a scheduled amount of active and reactive power. A protected unload circuit in DC link is adopted to help the integrated DFIG LVRT. This LVRT method increases the overload capacity of the DC capacitor, so that the decoupling control of active power and reactive power of DFIG are guaranteed by the rotor side converter, and the integrated DFIG-WF is not cut off from the grid during the transients. The detailed parameters of the test system and the

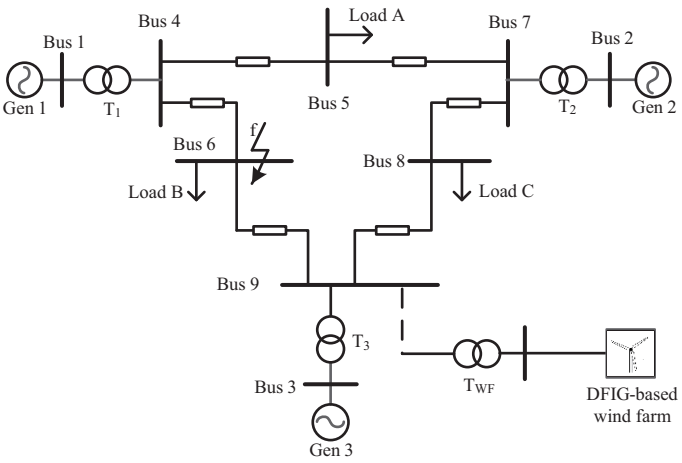

Fig. 1. Schematic of the 3-generator and 9-bus power system (with DFIG-based wind farm integrated).

integrated DFIG-WF are provided in Table AI and Table AII in the Appendix.

The variables considered for comparative simulations in this paper are DFIG capacity, access location, and replacement of synchronous generator, as listed in Table I. In these simulations, the system total power loads remain the same with and without the DFIG integration. The occurrence of a three-phase short-circuit fault at bus 6 at 2.0 s and lasting 0.15 s before clearance is simulated. A base case carried out on the original system with no DFIGs is set as the reference for comparisons.

TABLE I
SIMULATION SCENARIOS

Scenarios	Variables	Details of the Comparison
Scenario 1	DFIG capacity	30 MW DFIG-WF integrated at bus 9 60 MW DFIG-WF integrated at bus 9
Scenario 2	DFIG access location	30 MW DFIG-WF integrated at bus 4 30 MW DFIG-WF integrated at bus 7 30 MW DFIG-WF integrated at bus 9
Scenario 3	Replacement of synchronous generator	Gen 3 is replaced by same-capacity DFIGs equipped with SVC.

A. Impact on Transient Stability of the COI

1) Scenario 1

This section mainly focuses on how the COI's dynamic motion is influenced by the integrated DFIG-WF. In this scenario, a DFIG-WF is integrated into the test system in parallel with generator G_3 at bus 9 with no synchronous generators replaced. The rated capacity of DFIG-WF is set to 30 MW and 60 MW. With the above-described DFIG integration, changes in the network structure and the system dynamic voltage stability are negligible, and as such the system dynamic power demand can be regarded as unchanged according to (14). Based on (10)–(14), the variation of the three key factors that determine the COI's dynamic motion can be described by

$$\begin{cases} T'_{\mathrm{J,COI}} = T_{\mathrm{J,COI}} \\ P'_{\mathrm{m,COI}} = P_{\mathrm{m,COI}} - P_{\mathrm{m,DFIG}} \\ P'_{\mathrm{e,COI}} = P_{\mathrm{e,COI}} - P_{\mathrm{e,DFIG}}. \end{cases} \tag{18}$$

According to (4), (9), and (18), the changes in the COI's accelerating speed with DFIG integration is then written as

$$\begin{aligned} p(\omega'_{\mathrm{COI}}) - p(\omega_{\mathrm{COI}}) &= \frac{1}{T'_{\mathrm{J,COI}}} P'_{\mathrm{COI}} - \frac{1}{T_{\mathrm{J,COI}}} P_{\mathrm{COI}} \\ &= \frac{1}{T_{\mathrm{J,COI}}} (P_{\mathrm{e,DFIG}} - P_{m,DFIG}). \end{aligned} \tag{19}$$

DFIG's accelerating power $\Delta P_{\mathrm{DFIG}} = P_{\mathrm{m,DFIG}} - P_{\mathrm{e,DFIG}}$, is also expressed in terms of the difference in the COI's accelerating power

$$P'_{\mathrm{COI}} - P_{\mathrm{COI}} = -\Delta P_{\mathrm{DFIG}}. \tag{20}$$

According to (19), since the COI inertia constant is not been changed, the transient power response of the integrated DFIG-WF becomes the dominant factor affecting the COI's dynamic motion when DFIGs are integrated without replacing any synchronous generators. Fig. 2 shows the transient response of DFIG-WF's electrical power $P_{\mathrm{e,DFIG}}$ and accelerating power ΔP_{DFIG} with the rated capacity of 30 MW and 60 MW. It can be seen that as the DFIG-WF's capacity increases, the absolute value of DFIG-WF's accelerating power also increases both during the fault period and post-fault period whilst the absolute value of P'_{COI} decreases as shown in Fig. 3(a). This observation is consistent with (20). As indicated by (19), the COI's rotor speed ω'_{COI} exhibits lower accelerated speeds in both the accelerating process during the fault period and decelerating process during the post-fault period with larger DFIG's integrated capacity, which is shown in Fig. 2(b).

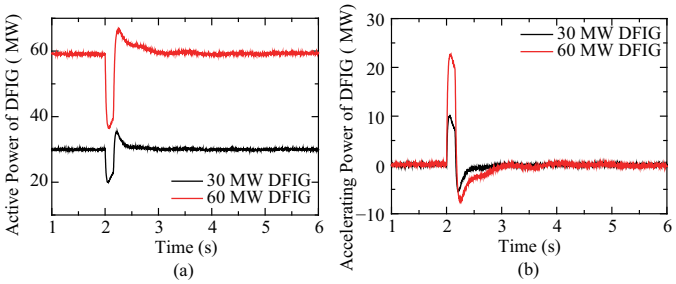

Fig. 2. Transient dynamics of (a) DFIG-WF's active power and (b) DFIG-WF's accelerating power.

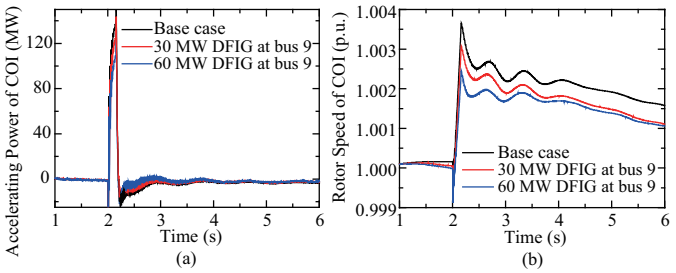

Fig. 3. Transient dynamics of the (a) COI's accelerating power and (b) COI's rotor speed.

2) Scenario 2

In this scenario, the influence of different access locations of the integrated DFIG-WF on the COI's dynamic motion is investigated. Specifically, a 30 MW DFIG-WF is integrated at one location of bus 4, bus 7, and bus 9 with no synchronous generator replaced. The formulations in (18)–(20) remain valid for this scenario.

Fig. 4 presents the transient response of DFIG-WF's terminal voltage U_{DFIG}, and accelerating power ΔP_{DFIG}. As presented in Fig. 4(a), it can be seen that under the same system disturbance, the different access locations of integrated DFIG-WF lead to different electrical distances from the DFIG-WF to the fault, which results in the disparities in the dynamic response of the DFIG's terminal voltages during the fault for the three different locations. This explains the difference in ΔP_{DFIG} as shown in Fig. 4(b), since DFIG's electrical power output is greatly influenced by the terminal voltage's dynamics.

Fig. 5(a) and Fig. 5(b) depict the dynamic response of the COI accelerating power P'_{COI} and the COI rotor speed ω'_{COI}

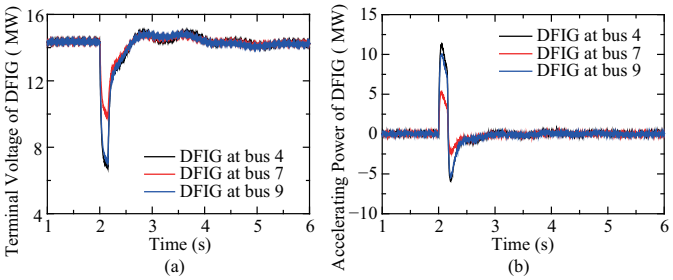

Fig. 4. Transient dynamics of (a) DFIG-WF's terminal voltage and (b) DFIG-WF's accelerating power.

during the transient process. Although the disparities of the dynamic response of P'_{COI} among the three cases are small, it still varies with the dynamics of the DFIG-WF's accelerating power output. In Fig. 5(b), the dynamics of COI rotor speed ω'_{COI} also stays in tight accordance with the variation trend of P'_{COI}.

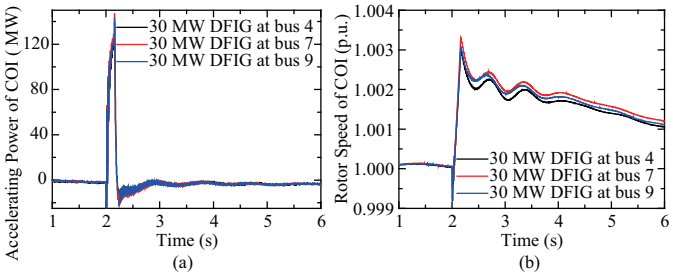

Fig. 5. Transient dynamics of the (a) COI's accelerating power and (b) COI's rotor speed.

3) Scenario 3

To investigate the impact of the changes in COI inertia constant on the COI's transient dynamics, the synchronous generator is considered. The synchronous generator G_3 is replaced by a DFIG-WF of the same rated active power capacity. The integrated DFIG's influence on system transient voltage stability is eliminated by equipping it with a fixed capacitor and a switched SVC. The fixed capacitor delivers static reactive power output and the switched SVC adjusts its reactive power output based on the terminal voltage sags [29]; thus the lack of dynamic reactive power caused by the replacement of G_3 is compensated.

Hence, with the above DFIG integration, the system dynamic power demand is regarded as unchanged. Compared with (18), only the conditions of COI's inertia constant is changed, and described as

$$T'_{\mathrm{J,COI}} = T_{\mathrm{J,COI}} - T_{\mathrm{J,G_3}}. \tag{21}$$

The COI's dynamic motion is then affected, together, by changes in the COI accelerating power P'_{COI}, and the COI inertia constant $T'_{\mathrm{J,COI}}$, expressed as

$$p(\omega'_{\mathrm{COI}}) = \frac{1}{T_{\mathrm{J,COI}} - T_{\mathrm{J,G_3}}}[(P_{\mathrm{m,COI}} - P_{\mathrm{e,COI}}) - \Delta P_{\mathrm{DFIG}}]. \tag{22}$$

Fig. 6 illustrates the transient response of DFIG-WF's accelerating power ΔP_{DFIG}. Since the DFIG-WF's rate capacity (85 MW) is larger than the two cases in Scenario 1, the amplitude of ΔP_{DFIG} also increases. Fig. 7(a) shows the dynamic response of COI accelerating power P'_{COI}. During the fault and post-fault periods, the absolute value of P'_{COI} drops substantially when compared to the base case, of which the deviation equals to the negative value of the DFIG-WF's accelerating power. However, in Fig. 7(b), ω'_{COI} does not present as much an influence as P'_{COI} when compared with the base case, both during the fault and after the fault. This is seen as being caused by reduced COI's inertia constant, since the COI's dynamic motion is influenced by the changes in $T'_{\mathrm{J,COI}}$ and P'_{COI} together according to (22).

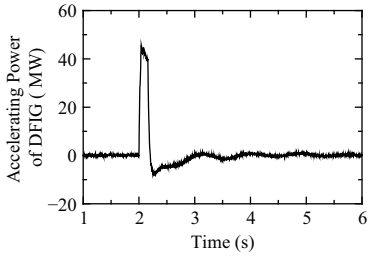

Fig. 6. Transient dynamics of DFIG-WF's accelerating power.

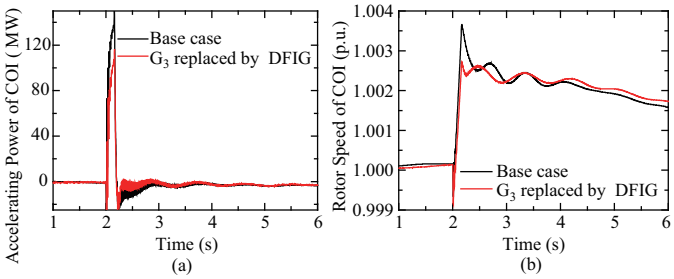

Fig. 7. Transient dynamics of the (a) COI's accelerating power and (b) COI's rotor speed.

4) Discussion

According to the analysis in Section IV and these three comparison simulations conducted above, the influence mechanism of integrated DFIGs on the general trend of the overall system is explored. It suggests that with the DFIG integration, the total amount of the dynamic electrical power output of the synchronous generators in the system is shared by the integrated DFIGs, which results in lower absolute values in COI's accelerating power during both the fault and post-fault periods. Hence, this influence is mainly affected by the integrated DFIG's power response characteristics, capacity and access locations. When DFIGs are integrated without replacing synchronous generator, the COI's acceleration power is the only factor affecting the COI's dynamic motion. However, when some of the synchronous generators are replaced, the influence from the changes in the COI's inertia constant also needs to be considered.

In addition, if considering the situation that the system transient voltage stability is changed by DFIG integration, the variations in the COI dynamic motion cannot be easily evaluated theoretically. This is because the changes in the

system transient voltage stability may lead to a different dynamic response of the system's power demand and generators' electrical power output.

B. Influence on the Transient Stability of Individual Synchronous Generators

1) Scenario 1

Based on the analysis of the influence of integrated DFIGs on the COI's dynamic motion in the last section, the influence on the dynamics of each individual synchronous generator with respect to the COI is considered in this section. Fig. 8 compares the rotor speed dynamics of each synchronous generator with respect to the COI in the two cases of Scenario 1 with the base case. It can be seen that though the accelerating speed of the rotor speed of the COI declines with the DFIG integration, as shown in Fig. 3(b), the influence on three generators' rotor speeds with respect to the COI are not all positive. With greater DFIG penetration, the rotor speeds of G_1 and G_3 have smaller fluctuations with respect to COI compared to the base case, whereas the rotor speed of G_2 is greater.

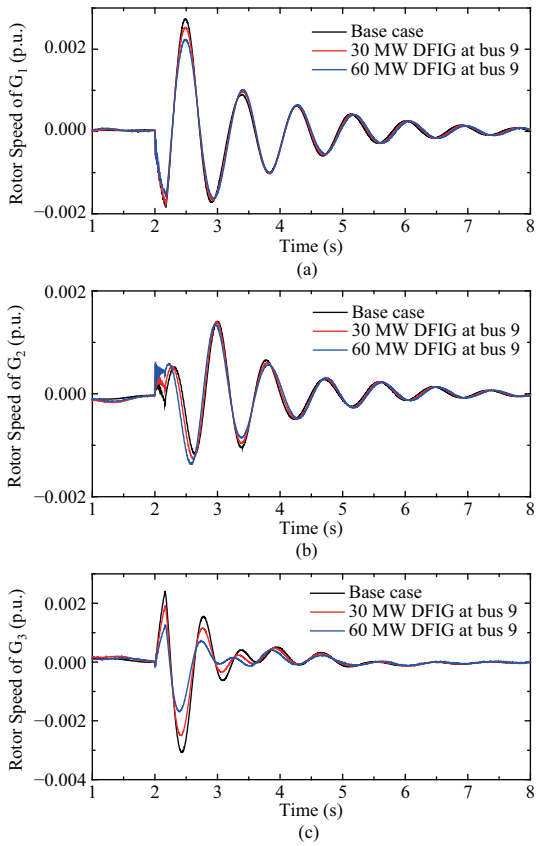

Fig. 8. Rotor speed dynamics of (a) G_1, (b) G_2 and (c) G_3 with respect to the COI.

Fig. 9(a) shows the steady-state rotor angle (SSRA) of each synchronous generator with respect to the COI at the pre-fault period. With the DFIG-WF integrated at bus 9, in parallel with G_3, the SSRA of G_3 declines the most among the three synchronous generators, resulted from that the electrical power output of G_3 is shared by the integrated DFIG-WF. Fig. 9(b) shows the peak value of the first swing of the rotor angle of the synchronous generator (PVFS) with respect to the COI after fault, which is defined as $(\delta_{i,\mathrm{FS}}^{\mathrm{COI}'} - \delta_{i,|0|}^{\mathrm{COI}'})$. It can be seen that when the DFIG capacity increases, the variations in the PVFS of the three synchronous generators show trends similar to the rotor speed.

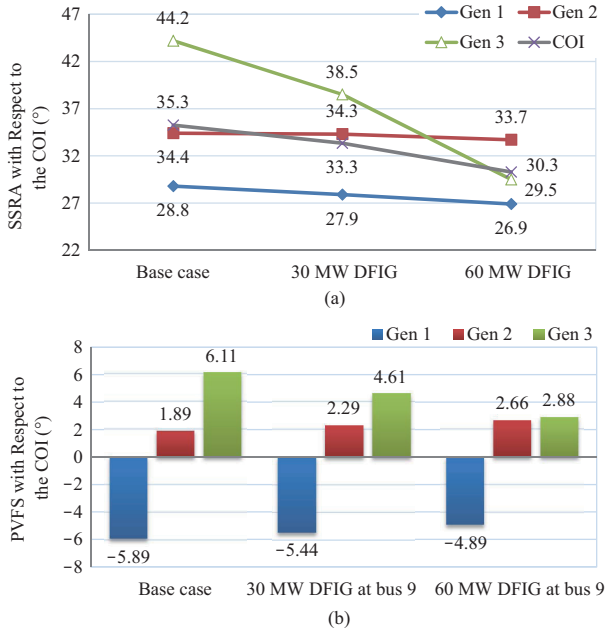

Fig. 9. SSRA and PVFS of each synchronous generator with respect to the COI. (a) SSRA. (b) PVFS.

2) Scenario 2

In this scenario, the integrated DFIG-WF's access location is considered. Fig. 10 presents the rotor speed dynamics of each synchronous generator with respect to the COI. It shows that although the COI's accelerating speed differs slightly with different DFIG integration locations as shown in Fig. 5(b), its influence on the three generators' rotor speeds with respect to the COI are not uniform: when DFIGs are integrated at bus 4, the three synchronous generators' rotor speeds all experience greater fluctuations with respect to the COI compared to the base case; when DFIGs are integrated at bus 7, the fluctuations in the rotor speeds of the three synchronous generators' are smaller than the base case; and when DFIGs are integrated at bus 9, the rotor speed dynamics, which has been described in Scenario 1, are also different from the last two cases.

Fig. 11(a) shows the SSRA of each synchronous generator with respect to the COI with different DFIG access locations. It shows that the SSRA of the synchronous generator, which is nearest to the DFIG's access point, declines the most. It also can be seen that when the SSRA of G_1 declines the most at the lowest operating point in the rotor angle, the dispersion of three generators' SSRA with respect to the COI experiences the greatest extension trend, and vice versa. The PVFS of the three synchronous generators with respect to the COI in the three comparison cases and the base case are presented in Fig. 11(b). The dispersion of these generators' PVFS values with respect to the COI shows a similar trend in terms of variations

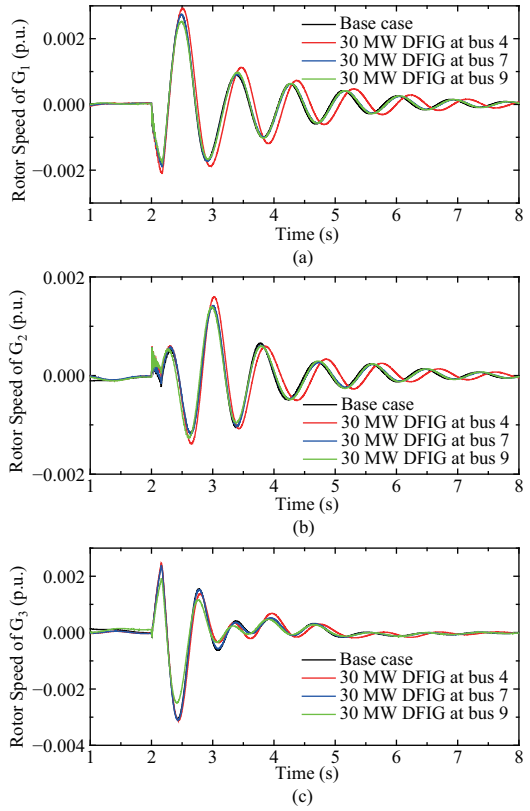

Fig. 10. Rotor speed dynamics of (a) G_1, (b) G_2 and (c) G_3 with respect to the COI.

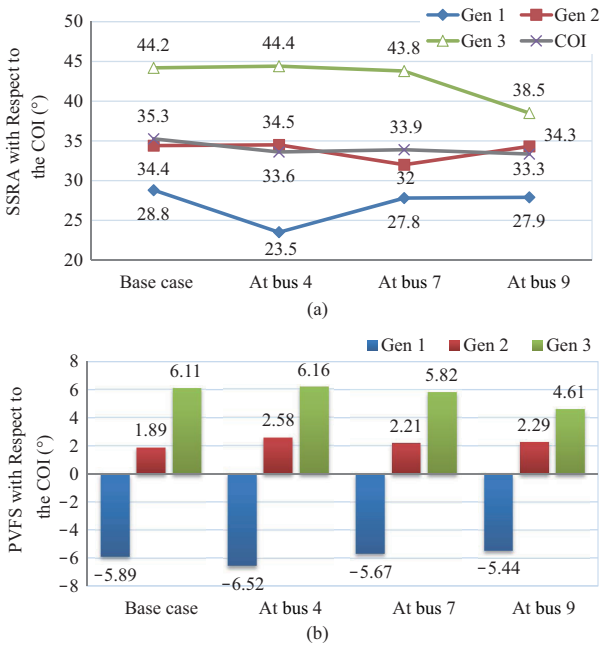

Fig. 11. SSRA and PVFS of each synchronous generator with respect to the COI. (a) SSRA. (b) PVFS.

as that of the SSRA, which indicates that the distribution of the generator's SSRA states also contributes to the transient fluctuations of PVFS with respect to the COI.

3) Scenario 3

In this scenario with G_3 replaced by integrated DFIG-WF, the rotor speed dynamics of the other two synchronous generators G_1 and G_2 with respect to the COI in this comparison case and the base case are shown in Fig. 12. It is observed that, with the DFIG integration, the fluctuation in the rotor speed of G_1 with respect to the COI is smaller than the base case. In contrast, the fluctuation in that of G_2 is slightly greater than the base case.

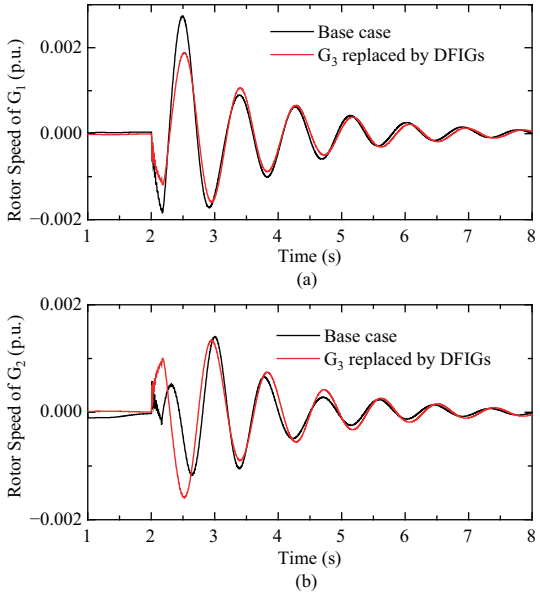

Fig. 12. Rotor speed dynamics of (a) G_1 and (b) G_2 with respect to the COI.

Fig. 13 shows the SSRA and PVFS of G_1 and G_2 with respect to the COI. With G_3 replaced, the synchronous genera-

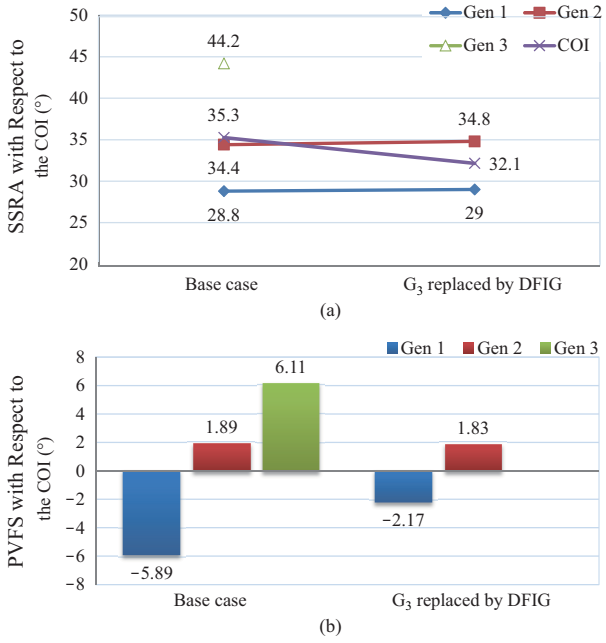

Fig. 13. SSRA and PVFS of each synchronous generator with respect to the COI. (a) SSRA. (b) PVFS.

tors in the system have formed a new COI, which is composed of G_1 and G_2 only. Hence, the SSRAs of G_1 and G_2 change as shown in Fig. 13(a), and in Fig. 13(b), and the PVFS of G_1 is significantly reduced with respect to the new COI whilst the PVFS of G_2 changes little. The replacement of the synchronous generator not only changes the total amount of system inertia and the dynamic power distribution, but also reforms the transient stability mode of the synchronization mechanism among synchronous generators.

4) Discussion

By undertaking simulations of these three scenarios, we can better understand the influence of integrated DFIGs on individual synchronous generator's rotor dynamics. The effects on rotor dynamics of different synchronous are not always the same. When the COI's rotor speed declines, the rotor speed of each synchronous generator with respect to the COI may decline, or not, depending on the dynamic motion of both the COI and the generator itself.

Compared with the COI, the dynamic variation of each synchronous generator's transient trajectories are affected more by the access location of the integrated DFIGs, since the synchronous generator's rotor dynamic is quite sensitive to the changes in system power distribution. However, this influence on the COI's electrical power is usually small. It indicates that when the integrated DFIGs' access location is near the synchronous generator, which operates with the top steady-state rotor angle, the dispersion of all the synchronous generators' rotor angle values will be reduced, and the fluctuations of the relative swings among the synchronous generators also decline.

VI. Conclusion

This work contributed to a better understanding of the influence mechanism of integrated DFIGs on power system transient stability. Based on the analysis of DFIG's transient behavior, the influence of integrated DFIGs on the dynamic motion of the COI system, the rotor speed and the rotor angle dynamics of each synchronous generator, with respect to the COI are qualitatively investigated. A comparative study using simulations that factor DFIG capacity, access location, and replacement of synchronous generator is conducted for further validation.

It is demonstrated that the dynamics of the COI and individual synchronous generators are influenced by the integrated DFIGs via different mechanisms, and are also sensitive to different variables in the DFIG's integration condition. The COI's transient dynamics, which is determined by the variations in the COI's inertia constant, and mechanical power and electrical power caused by DFIG integration, is affected more by the DFIG's transient power response and whether the synchronous generator is replaced. On the other hand, the rotor speed and rotor angle dynamics of each individual synchronous generator with respect to the COI, which are determined by the transient dynamics of both the COI and the generator itself, are influenced significantly by the system's power distribution, which varies with different access locations of the DFIGs.

The results of this work can also be instructive for research on DFIG's dynamic control to improve the system transient stability. In further research, the impacts of transient voltage stability will be considered for more comprehensive explanations.

Appendix

TABLE AI
Basic Parameters of the 3-generator and 9-bus Power System

Variables	Values (Gen 1)	Values (Gen 2)	Values (Gen 3)
Terminal voltage, U_N	16.5 kV	18.0 kV	13.8 kV
Generator inertia, T_J	5.62 s	6.67 s	4.7 s
Rated active power, P_N	105 MW	163 MW	85 MW
Rated reactive power, Q_N	43.7 MVar	38.6 MVar	15 MVar
Variables	Values (Load A)	Values (Load B)	Values (Load C)
Rated active power, P_N	142 MW	100 MW	103 MW
Rated reactive power, Q_N	56 MVar	35 MVar	34 MVar

TABLE AII
Parameters of Aggregated DFIG-based Wind Farm

Variables	Values
Terminal voltage, U_N	13.8 kV
Generator inertia, T_J	0.7267 s
Stator Reactance, R_s	0.0054 p.u.
Rotor Reactance, R_r	0.00607 p.u.
Magnetizing inductance, L_m	4.362 p.u.
Stator leakage inductance, L_{ls}	0.102 p.u.
Rotor leakage inductance, L_{lr}	0.11 p.u.

References

[1] L. P. Jiang, Y. N. Chi, H. Y. Qin, Z. Y. Pei, Q. H. Li, M. L. Liu, J. H. Bai, W. S. Wang, S. L. Feng, W. Z. Kong, and Q. K. Wang, "Wind energy in China," *IEEE Power and Energy Magazine*, vol. 9, no. 6, pp. 36–46, Dec. 2011.

[2] H. Chen, J. Li, F. Han, and H. Bai, "Power grid is getting ready for the development of wind power in China," in *Proceedings of IPEC*, 2010, pp. 396–401.

[3] Y. Feng, H. Y. Lin, S. L. Ho, J. H. Yan, J. N. Dong, S. H. Fang, and Y. K. Huang, "Overview of wind power generation in China: Status and development," *Renewable and Sustainable Energy Reviews*, vol. 50, pp. 847–858, Oct. 2015.

[4] M. Rahimi and M. Parniani, "Dynamic behavior analysis of doubly-fed induction generator wind turbines—the influence of rotor and speed controller parameters," *International Journal of Electrical Power & Energy Systems*, vol. 32, no. 5, pp. 464–477, Jun. 2010.

[5] A. A. B. M. Zin, P. H. A. Mahmoud, A. B. Khairuddin, L. Jahanshaloo, and O. Shariati, "An overview on doubly fed induction generators' controls and contributions to wind based electricity generation," *Renewable and Sustainable Energy Reviews*, vol. 27, pp. 692–708, Nov. 2013.

[6] K. Elkington, V. Knazkins, and M. Ghandhari, "On the stability of power systems containing doubly fed induction generator-based generation," *Electric Power Systems Research*, vol. 78, no. 9, pp. 1477–1484, Sep. 2008.

[7] H. Li, B. Zhao, C. Yang, H. W. Chen, and Z. Chen, "Analysis and estimation of transient stability for a grid-connected wind turbine with induction generator," *Renewable Energy*, vol. 36, no. 5, pp. 1469–1476, May 2011.

[8] N. Modi, T. K. Saha, and T. Anderson, "Damping performance of the large scale Queensland transmission network with significant wind penetration," *Applied Energy*, vol. 111, pp. 225–233, Nov. 2013.

[9] M. V. A. Nunes, J. A. P. Lopes, H. H. Zurn, U. H. Bezerra, and R. G. Almeida, "Influence of the variable-speed wind generators in transient stability margin of the conventional generators integrated in electrical grids," *IEEE Transactions on Energy Conversion*, vol. 19, no. 4, pp. 692–701, Nov. 2004.

[10] H. Hou, L. Lin, T. Wu, and Y. Z. Miao, "Comparison of transient stability between wind farm based on DFIG and traditional power plant in an actual grid," in *Proceedings of IEEE Power and Energy Engineering Conference*, 2010, pp. 1–4.
[11] Y. C. Zhang, J. Bank, E. Muljadi, Y. H. Wan, and D. Corbus, "Angle instability detection in power systems with high-wind penetration using synchrophasor measurements," *IEEE Journal of Emerging and Selected Topics in Power Electronics*, vol. 1, no. 4, pp. 306–314, Oct. 2013.
[12] S. Sheri, B. Shankarprasad, V. V. Bhat, and S. Jagadish, "Effect of doubly fed induction generator on transient stability analysis of grid," in *International Conference on Power Systems, ICPS*, 2009, pp. 1–6.
[13] A. Ramkumar and S. Durairaj, "An analysis of transient characteristics of interconnected DFIG with hydro governor synchronous generator," *IEEE Power, Signals, Controls and Computation (EPSCICON),* 2012, pp. 1–10.
[14] W. Qiao, R. G. Harley, and R. G. Harley, "Effect of grid-connected DFIG wind turbines on power system transient stability," in *Proceedings of IEEE Power and Energy Society General Meeting*, 2008, pp. 1–7.
[15] D. Gautam, V. Vittal, and T. Harbour, "Impact of increased penetration of DFIG-based wind turbine generators on transient and small signal stability of power systems," *IEEE Transactions on Power Systems*, vol. 24, no. 3, pp. 1426–1434, Jul. 2009.
[16] M. A. Chowdhury, N. Hosseinzadeh, W. X. Shen, and H. R. Pota, "Comparative study on fault responses of synchronous generators and wind turbine generators using transient stability index based on transient energy function," *International Journal of Electrical Power & Energy Systems*, vol. 51, pp. 145–152, Oct. 2013.
[17] L. B. Shi, S. Q. Dai, Y. X. Ni, L. Z. Yao, and M. Bazargan, "Transient stability of power systems with high penetration of DFIG based wind farms," in *Proceedings of IEEE Power & Energy Society General Meeting*, 2009, pp. 1–6.
[18] A. Mitra and D. Chatterjee, "A sensitivity based approach to assess the impacts of integration of variable speed wind farms on the transient stability of power systems," *Renewable Energy*, vol. 60, pp. 662–671, Dec. 2013.
[19] J. C. Cepeda, J. L. Rueda, D. G. Colomé, and D. E. Echeverría, "Real-time transient stability assessment based on center-of-inertia estimation from phasor measurement unit records," *IET Generation Transmission & Distribution*, vol. 8, no. 8, pp. 1363–1376, Aug. 2014.
[20] H. Hashim, M. R. Zulkepali, Y. R. Omar, N. Ismail, I. Z. Abidin, and S. Yusof, "An analysis of transient stability using Center-of-Inertia: angle and speed," in *Proceedings of IEEE International Conference on Power and Energy*, 2010, pp. 402–407.
[21] Z. B. Du, Y. Zhang, L. Liu, and Y. X. Ni, "COI based frequency slow dynamics simulations of ACDC interconnected power system incorporating AGC," in *Proceedings of IEEE Power Engineering Society General Meeting*, 2007, pp. 1–7.
[22] P. Kundur, *Power System Stability and Control*. New York, USA: McGraw-Hill Professional, 1994, pp. 946–948.
[23] S. E. Stanton and D. R. Waggoner, "A center-of-inertia transform applied to transient responses of nonlinear power systems," in *Proceedings of the Twenty-First Annual North-American Power Symposium,* 1989, pp. 205–210.
[24] H. Q. Yi, S. J. Cheng, Z. B. Du, L. B. Shi, and Y. X. Ni, "Modeling and simulation on long-term dynamics of interconnected power system using area COI concept," *Electric Power Systems Research*, vol. 78, no, 8, pp. 1369–1377, Aug. 2008.
[25] Z. B. Du, Y. Zhang, Y. X. Ni, L. B. Shi, L. Z. Yao, and M. Bazargan, "COI-based back-stepping sliding-mode emergency frequency control for interconnected ACDC power systems," in *Proceedings of IEEE Power & Energy Society General Meeting*, 2009, pp. 1–6.
[26] Z. H. Hao, Y. X. Yu, and Y. Zeng, "Transient performance of DFIG power angle in wind farm and its control strategy," *Electric Power Automation Equipment*, vol. 31, no. 2, pp. 79–83, Feb. 2011.
[27] C. Feltes, S. Engelhardt, J. Kretschmann, J. Fortmann, F. Koch, and I. Erlich, "Comparison of the grid support capability of DFIG-based wind farms and conventional power plants with synchronous generators," in *Proceedings of IEEE Power & Energy Society General Meeting,* 2009, pp. 1–7.
[28] S. Zhao and N. K. C. Nair, "Behavior of doubly-fed induction generator unit during system disturbance," in *Australasian Universities Power Engineering Conference*, 2008, pp. 1–6.
[29] T. Ahmed, K. Nishida, K. Soushin, and M. Nakaoka, "Static VAR compensator-based voltage control implementation of single-phase self-excited induction generator," *Electric Power Systems Research*, vol. 78, no. 9, pp. 1477–1484, Sep. 2008.

Siwei Liu was born in Hebei Province, China. He received the B.E degree from North China Electrical Power University (NCEPU) in 2010. Since 2010, he started master-doctor continuous study and is currently working towards his Ph.D. degree in electrical engineering and automation in NCEPU. His research interest includes doubly-fed induction turbine modeling and transient response analysis, power system transient stability, and grid integration of DFIG-based wind power.

Gengyin Li (M'03) was born in Hebei Province, China. He received his B.S., M.S., and Ph.D. degrees, all in electrical engineering from North China Electricity Power University (NCEPU) in 1984, 1987, and 1996, respectively. Since 1987, Dr. Li has been with the School of Electrical and Electronic Engineering at NCEPU, where he is currently a Professor and Executive Vice Dean of the school. His areas of interest include power system analysis and reliability, power systems economics, power quality analysis and control, and HVDC and VSC-HVDC transmission technology.

Ming Zhou (M'06) was born in Hubei Province, China. She received the B.S., M.S., and Ph.D. degrees in electrical engineering from North China Electricity Power University (NCEPU) in 1989, 1992, and 2006, respectively. Since 1992, she has been with the School of Electrical and Electronic Engineering at NCEPU, where she is currently a Professor. Her research interests are power system analysis and reliability, power systems economics, and power quality analysis.